Effect of Substrates on the Infrared External Reflection Spectra of Langmuir–Blodgett Films

Takeshi Hasegawa,* Jujiro Nishijo, Yoshihiro Kobayashi,† and Junzo Umemura,††

Kobe Pharmaceutical University, Motoyama-kitamachi, Higashinada-ku, Kobe 658

†NTT Basic Research Laboratories, 3-1 Morinosato, Wakamiya, Atsugi, Kanagawa 243-01

††Institute for Chemical Research, Kyoto University, Uji, Kyoto 611

(Received May 15, 1996)

The Fourier transform infrared (FTIR) polarized external reflection (ER) spectra of 9-monolayer cadmium stearate Langmuir–Blodgett (LB) films were measured on various kinds of materials (Ge, ZnSe, and GaAs) in order to investigate whether their spectra could be used for a quantitative analysis of the molecular orientation. The FTIR ER spectra on double-side-polished substrates with LB films on both sides would not fit in, even qualitatively, with the 5-layer system (IR//air/LB/substrate/LB/air) theoretical prediction. On the other hand, the ER spectra of a single-side-deposited LB film (IR//air/substrate/LB/air) were qualitatively explained by a simple 3-layer system (IR//substrate/LB/air) in which the reflection in the substrate was treated as a single reflection. This indicated that the output rays from the substrate in the conventional 5-layer system did not interfere sufficiently with each other. A 5-layer system calculation without any interference effect qualitatively explained the ER spectra of LB films on a double-side-polished substrate. It was eventually concluded that double-side-polished materials are not suitable for a precise analysis of ER spectra, since it is almost impossible to estimate the area ratio of interferential and non-interferential rays.

Polarized FTIR ER spectroscopy has recently become a powerful tool for analyzing the molecular orientation of ultra-thin organic films on various substrates.[1,2] One reason for this is that the sensitivity of the FTIR instrument, itself, has been greatly improved, making it possible to measure the ER spectra of even monolayer films.[3,4] The theoretical basis needed to analyze the ER spectra, on the other hand, has not kept pace with technological developments. In earlier days, Hansen's optical theory for stratified layers,[5] in which the optical constant for each layer was assumed to be isotropic, was often used to calculate the absorbance in the polarized FTIR spectra of LB films. Transmission and reflection-absorption (RA) measurements[6,7] were the most popular techniques (RA measurements of films on metallic substrates and transmission measurements of films on infrared transparent substrates), and Hansen's isotropic theory was adaptable because the directivity of the electric-field vectors of infrared beams on the substrate surface was very strong in these techniques.[6] When the directivity of the electric field is not strong, on the other hand, the electric field strongly reflects the optical anisotropy in each phase.[2] The optical conditions, like this, often take place on non-metallic substrates.[2] Thus, the isotropic approximation theory in its original form, could not be applied[8] to the ER measurements of non-metallic substrates. Optical anisotropy should therefore be used in calculations concerning this system. Some theories have been proposed to calculate the reflection-absorbance of the ER spectra with anisotropic optical constants.[1,2] Yeh, for example, developed a rigorous 4×4 transfer matrix theory for multi-layered anisotropic films;[9] further, Parikh and Allara used Yeh's matrix to develop a powerful calculation algorithm,[1] with which they reproduced the RA spectra of the octadecyl mercaptan monolayer on a polycrystalline gold (1 1 1) surface. Hasegawa et al. later proposed another estimation theory to analyze the ER spectra;[2] with that theory the uniaxial optical anisotropy in each phase could easily be taken in the conventional isotropic theory. In that work, the polarized ER spectra of a 9-monolayer Langmuir–Blodgett (LB) film of cadmium stearate on a gallium arsenide (GaAs) wafer were measured, and the molecular orientation determined from the spectra was quantitatively consistent with the results of a X-ray analysis. Both the measurement technique and the analyzing method were prepared based on the above consideration, and both were expected to provide a way to analyze the molecular orientation of ultra-thin films on any material. However, we occasionally encountered cases where even this anisotropic theory could not reproduce the ER spectra measured on IR-transparent substrates. We recently found that an LB film prepared on a substrate with two surfaces finely polished to a mirror finish gave an extraordinary reflection-absorbance far above the theoretical prediction. There have been no studies concerning the discrepancy between theoretical calculations and the observations of LB films on double-side-polished substrates.

We therefore investigated the reasons for such a discrepancy. We did this by measuring the ER spectra of 9-monolayer LB films of cadmium stearate on various substrates—namely a germanium attenuated-total-reflection (ATR)[10]

plate, a zinc selenide ATR plate, and a GaAs wafer—and by analyzing the optical system around the films. The results of this analysis showed that an accurate IR-ER analysis is impossible when the LB film is on a substrate made of an IR-transparent material with double-sided polished surfaces.

Experimental

The pure stearic acid used in this study was the same as that already reported in an earlier study.[11] Distilled water was produced using a modified Mitamura Riken Model PFL-DSR automatic lab still comprising a reverse-osmosis module, an ion-exchange column, and a double distiller. The cadmium chloride was a guaranteed reagent purchased from Wako Pure Chemical Industries Ltd., and was used without further purification. Langmuir films of cadmium stearate were prepared by spreading a solution of stearic acid in benzene (1.0 mg mL^{-1}) on the surface of an aqueous solution of 3×10^{-4} M $CdCl_2$, (1M = 1mol dm^{-3}), whose pH was controlled to pH 6.2 with 3×10^{-4} M $NaHCO_3$. After 10 min (to allow all of the solvent to evaporate), the film was transferred onto a substrate: either a finely polished GaAs circular wafer (50 mm diameter, 0.5 mm thick), or on an ATR plate (52×18×2 mm) made of Ge or ZnSe. The ATR plates had been purchased from Pier Optics Co., Ltd., Tatebayashi, Gunma, and had also been cleaned ultrasonicly in ethanol, acetone, and dichloromethane (successively for 10 min each) at 20 °C before a transfer of the monolayers was carried out by the conventional LB method[12] at a surface pressure of 30 mN m^{-1}. The dipping and withdrawal speeds of the wafers were 5 mm min^{-1}, and the transfer ratio was 0.97±0.05 throughout the experiments. To prepare a single-side built LB film on a ZnSe ATR plate, the edges of two ZnSe ATR plates were first adhered together with silicone rubber (type RTV made by Shin-Etsu Chemical Co., Ltd.). The Langmuir films were transferred to the stuck plate, and after the plates dried they were separated to form two pieces of single-sided built LB film. A single-sided-polished ZnSe substrate was purchased from Ohyo Koken Kogyo Co., Ltd., Tokyo. The unpolished surface of this substrate was very coarse, and looked white.

The FTIR ER spectra were recorded on a Nicolet Model 710 FTIR spectrophotometer equipped with an MCT detector. The resolution was 4 cm^{-1}. For reflection measurements, a Harrick Model RMA-1DG/VRA reflection attachment was used. The *p*-polarized and *s*-polarized IR beams were obtained through a Hitachi wire-grid polarizer, and the number of interferogram accumulations was 5000 for all of the measurements.

Atomic-force microscope (AFM) measurements for evaluating the surfaces of the substrates were performed in the tapping mode on a NanoScope III (Digital Instruments).

Theoretical

The theory used in this study for calculating the reflection-absorbance in the IR ER spectra of LB films was the same as that reported previously.[2] It is based on Hansen's isotropic optical theory for stratified layers,[5] and incorporates the uniaxial anisotropy in each phase according to Drude's anisotropic theory for a 2-layer system.[13] Using the cited anisotropic optical constants in each phase in the LB films, the reflection-absorbance was calculated. Other calculations are mentioned in the next section. The calculation process was coded in Fortran77 language compiled by the Language System Co., LS-FORTRAN, compiler on an Apple Macintosh Centris 660AV personal computer with System 7.1. A high-precision calculation (complex*24) was performed for complex values.

Results and Discussion

We first measured the ER spectra of 9-monolayer cadmium stearate LB films on a Ge ATR plate. After the LB films were prepared by the ordinary LB method,[12] both surfaces of the substrate were covered with 9-monolayer films. The surfaces had been polished with diamond paste for optical use, such as that used for ATR measurement.[10] The system used for an ER measurement with this substrate is schematically shown in Fig. 1. The angles of incidence for the *s*- and *p*-polarized beams were, respectively, 30° and 70°. This angle for *p*-polarization measurements was selected to make the ER measurements highly sensitive, since the Brewster angle was about 76°.[2] The obtained spectra (Fig. 2) show an outstanding feature: All bands show positive reflection-absorbances, irrespective of the polarization. These positive reflection-absorbances could not be explained by a simple 3-layer (IR//air/LB/substrate) model.[2] According to a 3-layer system calculation, the bands in the *s*-polarization spectra should always show negative reflection-absorbances irrespective of the angle of incidence. This implies that the ER spectra in Fig. 2 were affected not only by the film on the top side, but by the film on the opposite side. In order to take the signal from the reflections at the opposite side into account, a 5-layer (IR//air/LB/Ge/LB/air) model is necessary to analyze the spectra. We then tried to reproduce the spectra by way of a 5-layer model calculation.

In the 5-layer model, the real parts of the uniaxial refractive indices for LB film layers on a Ge ATR plate (the 2nd and 4th layer) were set at $n_{2o}=n_{4o}=1.48$ and $n_{2e}=n_{4e}=1.56$.[14,15] The subscripts o (ordinary ray) and e (extraordinary ray) here, respectively, refer to the surface-parallel and surface-normal directions.[2] The imaginary part of the complex refractive indices (the extinction coefficient) in bulk (k_{bulk}) of the $\nu_s(CH_2)$ mode in a stearyl group at 2850 cm^{-1} is already known to be 0.2 at room temperature.[18] For the present calculation, the molecular orientation in the cadmium stearate LB film was assumed to be the same as the molecular orientation on an amorphous surface.[7] Since the surface of the ATR plate was considered to be covered with an amorphous-like oxide layer, this assumption may be appropriate. The orientation angles for the transition moments of the $\nu_a(CH_2)$, $\nu_s(CH_2)$, and $\nu_s(COO^-)$ vibration bands were then, respectively, determined to be 85°, 85°, and 18° from the surface normal.

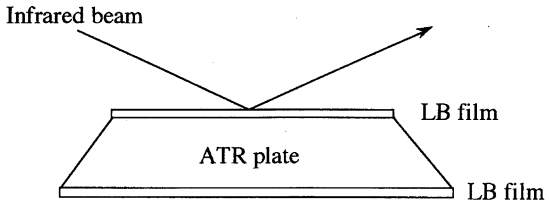

Fig. 1. Scheme for the infrared ER measurement of LB films on ATR plates.

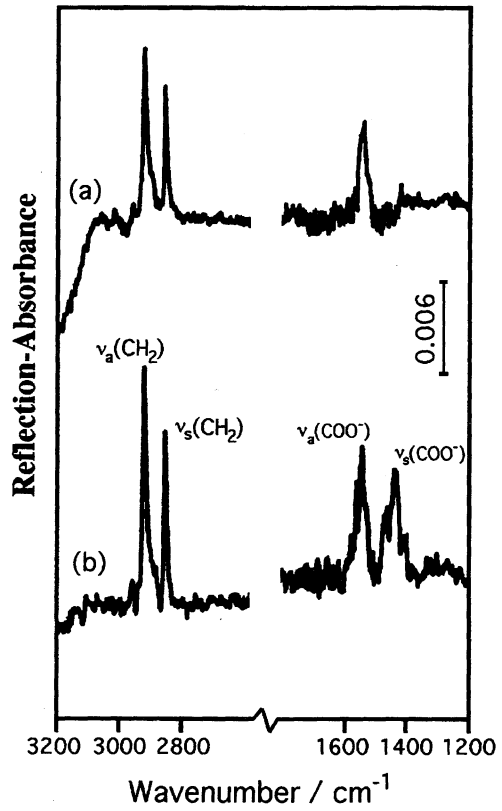

Fig. 2. Infrared ER spectra of 9-monolayer LB films of cadmium stearate on both surfaces of a Ge ATR plate: (a) *s*-polarized beam, (b) *p*-polarized beam. (The angles of incidence were 30° and 70°, respectively.)

Since the $\nu_s(COO^-)$ mode had a big refractive index dispersion on the wavelength,[2] the calculation for this band is not discussed here. Then, the imaginary part of each refractive index was calculated by the following equations:[2]

$$k_{2o} = k_x = k_y = \frac{3}{2} k_{bulk} \sin^2 \phi, \quad (1)$$

$$k_{2e} = k_z = 3k_{bulk} \cos^2 \phi, \quad (2)$$

where ϕ is the orientation angle of the transition moment measured from the surface normal of the LB films. Each extinction coefficient (k_{bulk}) at 25 °C for the $\nu_a(CH_2)$ and $\nu_s(COO^-)$ modes was 0.264, and 0.110, respectively.[2] For the $\nu_s(CH_2)$ mode at 2850 cm^{-1}, for example, the anisotropic optical constants were calculated to be $\tilde{n}_{2o}=\tilde{n}_{4o}=1.48+0.2977i$ and $\tilde{n}_{2e}=\tilde{n}_{4e}=1.56+0.0046i$, where i is the square root of minus one. Variable with a tilde (~) has a complex value. The $\tilde{n}_3$ for the Ge substrate at various wavelengths was taken from other literature,[14,15] as 4.03 at 2917 and 2850 cm^{-1} and as 4.01 at 1443 cm^{-1}. Regardless of the wavenumber, the refractive index, $\tilde{n}_1$ or $\tilde{n}_5$ for the air phase, was 1.0 and the thicknesses of the phases were $h_2=h_4=22.5$ nm and $h_3=2.0$ mm. These constants were used to calculate the theoretical reflection-absorbance for each band;[2] these values are listed in Table 1. The calculated values are all positive, which is consistent with the spectra. The relative reflection-absorbances calculated from Table 1, however, are far from the relative ones in the spectra. These results indicate that the conventional 5-layer model calculation alone is not sufficient to analyze the spectra.

Table 1. Calculated Absorbances for *p*- and *s*-Polarization Measurements
The LB film was prepared on both sides of the Ge ATR crystal.

Band	Calculated absorbance	
	p-Pol. (70°)	*s*-Pol. (30°)
$\nu_a(CH_2)$	0.006602	0.006137
$\nu_s(CH_2)$	0.008278	0.021246
$\nu_a(COO^-)$	0.006235	0.011515
$\nu_s(COO^-)$	0.008403	0.000103

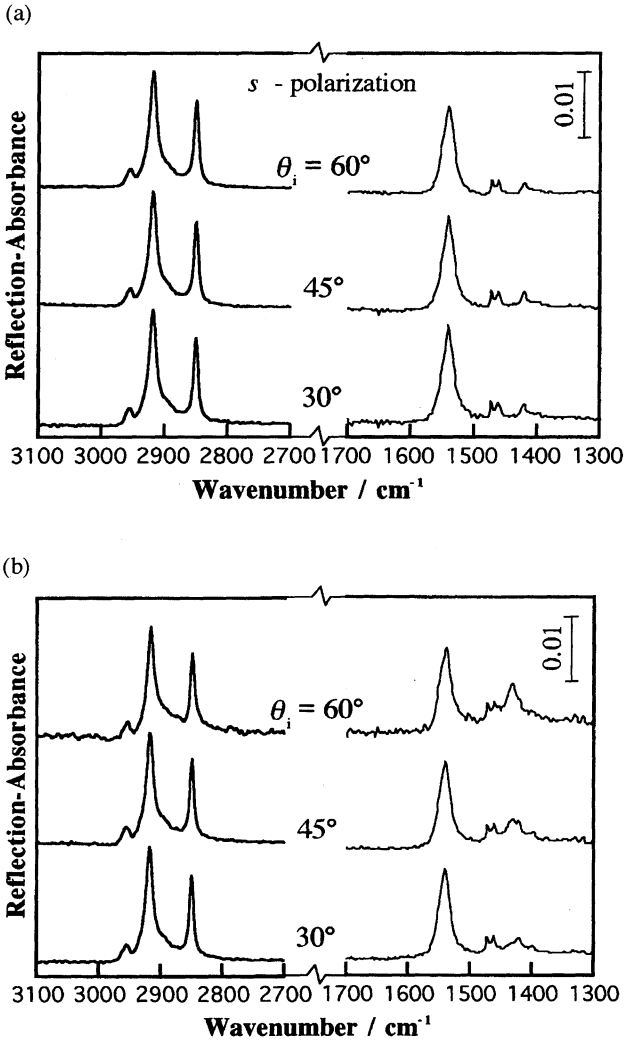

Fig. 3. Infrared ER spectra of 9-monolayer LB films of cadmium stearate prepared on both surfaces of a ZnSe ATR plate at angles of incidence of 30°, 45°, and 60° in (a) *s*-polarization and (b) *p*-polarization.

The large refractive index of Ge ($n\approx4.0$) may relate to an extraordinary spectrum or calculation. To check the effect of the refractive index of the substrate on the peak intensity, we also measured the ER spectra of the same film on a ZnSe

($n \approx 2.4$) ATR plate that had been finely polished, like the Ge plate. For this LB film, polarized ER measurements were employed at three angles of incidence: 30°, 45°, and 60°. The results are shown in Fig. 3(a) and (b) for *s*- and *p*-polarized beams, respectively. It is noteworthy that the three spectra in each polarization are quite similar in intensity to each other, while the COO^- stretching mode (1433 cm^{-1}) in *p*-polarization is apparently strengthened with the angle of incidence. They gave only positive peaks in both polarizations, like the spectra for Ge. The $\nu_s(COO^-)$ band was found to split slightly. There is a weak band at 1398 cm^{-1} that corresponds to the $\nu_s(COO^-)$ band of zinc stearate[16] as well as the $\nu_s(COO^-)$ band at 1433 cm^{-1} for cadmium stearate. This means that cadmium ions were partially replaced by zinc ions diffused from the substrate. Therefore, the COO^- stretching bands in the spectra may contain some experimental error.

Here, we used the same 5-layer model as that mentioned above to calculate the expected reflection-absorbance. The optical constants that we used for ZnSe were $\tilde{n}_3 =$ 2.435, 2.434, and 2.423 at 2917, 2850, and 1433 cm^{-1}, respectively.[15] The rest constants and the assumption of molecular orientation angles were the same as those in the case of Ge. The calculated results are shown in Fig. 4 along with the observed results against the angle of incidence. The observed reflection-absorbances are indicated by the broken lines, and the calculated ones by the solid lines. All of their features are similar to the conditions for the Ge plate being all positive (Table 1). However, the calculated values were found to be quite unstable upon changing the angle of incidence. As a result, the effect of the refractive index of the substrate was not a serious factor, and a conventional 5-layer model calculation alone was not sufficient to explain either the quantitative or qualitative results.

At this stage, we proposed two possible reasons that might cause the discrepancies between the experimental and calculated reflection-absorbances: 1) The first was that an unexpected multiple reflection might occur in the substrate due to the incompleteness of its architecture. Although the ATR plates should have been very finely fabricated, some inaccuracy in the surface finishing or parallelism of the surfaces may have remained. In thin film layers, multiple reflection takes place over a limited micro area, since the film is very thin compared to the wavelength. In the substrate, however, multiple reflection occurs over a much larger area because of the greater thickness. These multiple reflections over a large area might reflect the incompleteness of parallelism or surface finishing. 2) The second reason could be that the locations of the output signals shift from the incidental point, and may affect the measurement system in FTIR. This optical system is schematically shown in Fig. 5 where the thicknesses of LB films have been exaggerated in order to simplify the explanation. The refraction angle of the IR beam in the plate depends on the refractive index of the plate. At 2850 cm^{-1}, for example, the refractive index of Ge is approximately 4.03, and its refraction angle is thus 13.5° when the angle of incidence is 70°. On the other hand, since the refractive index of ZnSe at 2850 cm^{-1} is 2.43, the refraction angle should be 20.9° when the angle of incidence is 60°. Thus, the distances between the incidental point and the first output point on the Ge and ZnSe plates are 0.97 mm and 1.53 mm, respectively. In a practical system, the reflection in each phase is multiplied, as shown in Fig. 6. For simplicity, only the upper three layers (IR//air/LB/substrate) are shown. The

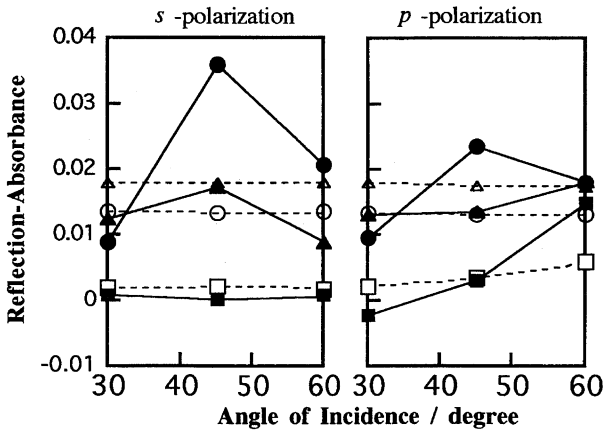

Fig. 4. Calculated (solid line) and measured (broken line) reflection-absorbances against the angle of incidence. The calculation was based on the conventional 5-layer model where all multiple reflections were taken into account. Squares, circles, and triangles indicate respective $\nu_a(CH_2)$, $\nu_s(CH_2)$, and $\nu_s(COO^-)$ modes.

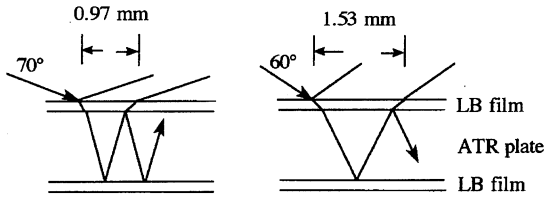

Fig. 5. Diagrams for the definition of distance shift between the incidental point and the first output point. The wave number, here, is 2850 cm^{-1} and the plate thickness is 2.0 mm.

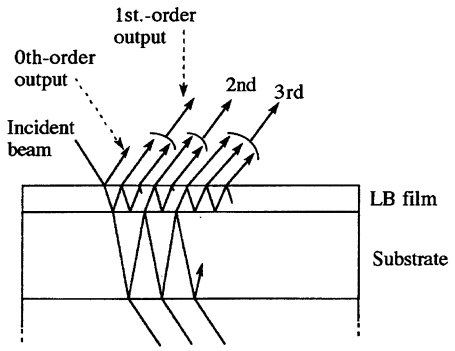

Fig. 6. A diagram for the definition of the order of reflected output. The thickness of the LB film is exaggerated to simplify explanation.

sum of the multiply-reflected beams that come from the first reflection on the *upper* surface of the substrate is defined here as the first-order output, and the sum of the multiply-reflected beams in the film phase that come from the first reflection on the *bottom* surface of the substrate is defined as the second-order output. The succeeding order outputs are also defined in Fig. 6. If the distance shift in Fig. 6 is taken into account, the shift from the incidental point would be larger at a higher-order output: to the millimeter order or more. In our optical system, some higher order output beams might miss the detector in the FTIR apparatus because of the large shift. As a result, the detected intensity of this high order output would be less than that expected. This would cause a difference between the experimental and theoretical results, because the calculation takes all multiple reflections and all outputs into account equally. For the two reasons mentioned, the calculation taking only low-order outputs into account is legitimately expected to fit the measured spectra. We next tried two other kinds of calculations.

At first, a calculation considering only a single-reflection in the substrate was carried out for the 5-layer model. A schematic diagram for the calculation is shown in Fig. 7(b). Only the single reflection was taken into account in the substrate, while multiple reflections were taken into account in the thin-film layers (Fig. 7(a)). $\tilde{R}_1$, $\tilde{R}_2$, $\tilde{T}_1$, and $\tilde{T}_1'$ in the diagram are, respectively, the reflection coefficients and the transmission coefficients at the interfaces of two film layers (Fig. 7(a)). The prime ($'$) means that the direction of the IR ray across the film layer is reversed. All of the coefficients were calculated by our method,[2] and the total amount of the reflection coefficient for a single reflection ($\tilde{r}$) was calculated by the following equation:

$$\tilde{r} = \tilde{R}_1 + \tilde{T}_1\tilde{R}_2\tilde{T}_1' \exp(-i\frac{4\pi}{\lambda}\tilde{n}_{2o}d\cos\phi). \quad (3)$$

Here, λ, $\tilde{n}_{2o}$, d, and ϕ are the wavelength, refractive index of the ZnSe substrate for ordinary rays, thickness of the substrate, and refraction angle in the substrate, respectively. Using this $\tilde{r}$, the reflection absorbance was calculated by the following equation, where $\tilde{r}_0$ is the reflection coefficient for LB films with no absorption:

$$A = -\log_{10}\frac{|\tilde{r}|^2}{|\tilde{r}_0|^2}. \quad (4)$$

The calculated result using the single-reflection model is summarized in Fig. 8. The calculated values for the *p*-polarization are slightly closer to the observed values than those using the multiple-reflection model (Fig. 4). However, the calculation is highly unstable, depending on the angle of incidence, especially for *s*-polarization. For example, the calculated reflection-absorbance for the $\nu_s(CH_2)$ mode for *s*-polarization at an angle of incidence of 45° is negative, which is quite different from the observed value. Since the measured reflection-absorbances were very stable on the angle of incidence, we can conclude that the single-reflection condition alone is inadequate explain the discrepancy between the calculation and the measurements. We thus tried another theoretical approach.

The new system is schematically shown in Fig. 9(a). This LB film comprises four phases (IR//air/ZnSe/film/air), where the IR beam was incident on the interface between air and ZnSe. All multiple reflections in both the film and the substrate are taken into account in this system. If multiple reflection in the substrate is neglected, on the other hand, we can reduce this 4-layer system to a simple 3-layer system

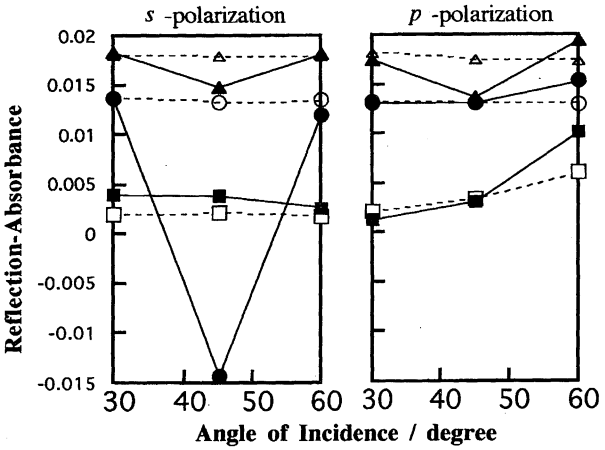

Fig. 8. Calculated (solid line) and measured (broken line) reflection-absorbances against the angle of incidence. The calculation was based on the single reflection model. Squares, circles, and triangles indicate respective $\nu_a(CH_2)$, $\nu_s(CH_2)$, and $\nu_s(COO^-)$ modes.

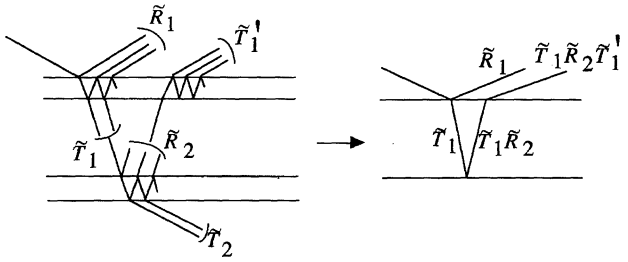

(a) Definition (b) Calculation

Fig. 7. Schematic diagram for single reflection calculation in 5-layer system. Multiple reflection was taken into account in the film layers. With the coefficients defined as in (a), the calculation was carried out as shown in (b).

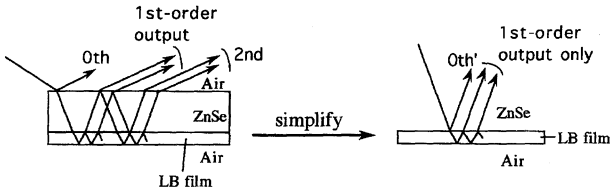

(a) 4-layer model (b) 3-layer model

Fig. 9. Schematic diagrams for (a) the 4-layer model and (b) the 3-layer model. The 4-layer model is reduced to the 3-layer model by extreme approximation whereby only the 0th-order and the first-order output reach the detector.

(Fig. 9(b)). This simplification is supported by the fact that there is no film layer on the upper surface. Although the 0th′-order output in this 3-layer system is not exactly the same as that in the system shown in Fig. 9(a), in an actual measurement the 0th-order output in a sample measurement is canceled by that in a reference measurement when the absorption in the film is sufficiently weak. The results of calculations for both the 4-layer system and the 3-layer system are listed in Table 2. There is a decisive difference between the two models in the reflection-absorbance for the $\nu_a(CH_2)$ band: according to the 4-layer model it is negative, whereas it is positive according to the 3-layer model. All of the bands in the measured polarized ER spectra of the single-side built LB film (Fig. 10) showed positive reflection-absorbances—except for the $\nu_s(COO^-)$ band. This corresponds fairly well to a prediction made based on the 3-layer model (Table 2). Since this model is an extreme approximation, the calculated values do not quantitatively agree with the experimental values; however, the relative intensities in the 3-layer calculation are almost perfectly consistent with the spectra measured for both polarizations. This calculation has merit not only because the higher-order outputs can be eliminated, but also because the thickness and refractive index of the substrate can be eliminated (Fig. 7(b)). This elimination of the physical parameters of the substrate greatly helps the calculated values to stabilize when the parameters are changed slightly. The conventional 5-layer (or 4-layer) calculation strongly depended on the physical condition of the substrate, since the thickness (far thicker than the wavelength) affected the phase term in Eq. 3. Since the actual measurements gave very stable and reproducible reflection-absorbances (Fig. 3(a), and (b)), the 3-layer model with no multiple-reflection was thought to be closer to the actual system than the 4-layer model, taking multiple-reflection into account. From our results and discussion, we can summarize that the single-reflection model with the 5-layer system and the multiple-reflection model in 4- or 5-layer systems all gave unstable results, whereas only the single-reflection model in the reduced 3-layer system gave very stable results whose relative intensity was consistent with the observed result. This difference can be understood by considering the interference among reflected rays. Only in the case of Fig. 9(b), the multiple-reflected rays strongly interfere with each other going to the detector, since the film layer is extremely thin. In other cases, however, the multiple-reflected rays cannot interfere completely, since they are somewhat separate from one another because of the thickness of the substrate. In this way, there is the possibility that a non-interferential calculation can explain the ER spectra, even with the 5-layer calculation.

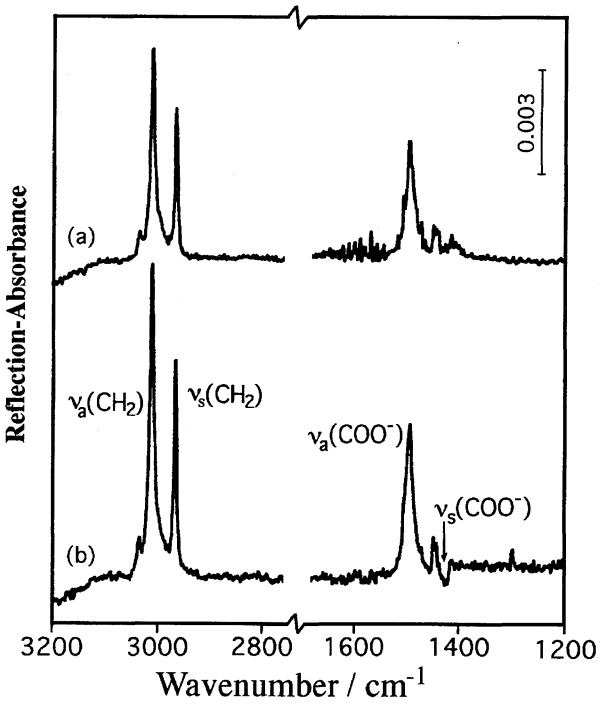

Fig. 10. Infrared ER spectra of a single-side built 9-monolayer LB film on a ZnSe ATR plate: (a) *s*-polarized beam, (b) *p*-polarized beam. Squares, circles, and triangles indicate respective $\nu_a(CH_2)$, $\nu_s(CH_2)$, and $\nu_s(COO^-)$ modes.

To obtain the sum of non-interferential outputs, each reflection coefficient should be squared individually; the squared values should be then added up.[17] The total amount of the reflection-absorption coefficient, $|\tilde{r}^*|^2$, for a non-interferential system can then be described as the following equation,[18] where $\tilde{r}^*$ is the reflection coefficient corresponding to the total amount of non-interferential output:

$$|\tilde{r}^*|^2 = \left|\tilde{R}_1\right|^2 + \left|\tilde{T}_1\tilde{R}_2\tilde{T}_1'\right|^2 + \left|\tilde{T}_1\tilde{R}_2^2\tilde{T}_1'\tilde{R}_1'\right|^2 + \left|\tilde{T}_1\tilde{R}_2^3\tilde{T}_1'\tilde{R}_1'^2\right|^2 + \cdots \quad (5)$$

The definition of each variable is given in Fig. 7(a). Since this equation does not converge analytically, we decided to sum up the first four terms. This approximation was sufficient to evaluate $\tilde{r}^*$. The results are summarized in Fig. 11. The calculated intensity was very stable even when the substrate

Table 2. Calculated Absorbances for *p*- and *s*-Polarization Measurements
The LB film was prepared on only one side of the ZnSe ATR plate, and the infrared beam was incident from the opposite side of the film.

Band	4-Layer model		3-Layer model	
	p-Pol.	*s*-Pol.	*p*-Pol.	*s*-Pol.
$\nu_a(CH_2)$	−0.009784	0.004996	0.051817	0.039285
$\nu_s(CH_2)$	0.012327	0.006945	0.038239	0.029058
$\nu_a(COO^-)$	0.013225	0.006830	0.025758	0.019623
$\nu_s(COO^-)$	−0.001842	0.000227	−0.003534	0.000777

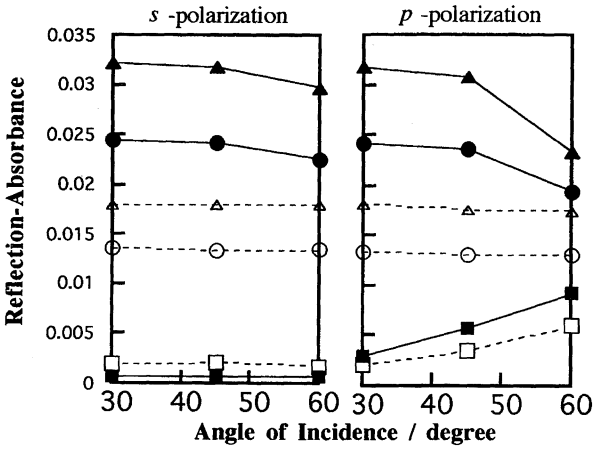

Fig. 11. Calculated (solid line) and measured (broken line) reflection-absorbances against the angle of incidence. Calculation was based on the non-interference model adapted to the 5-layer system. Squares, circles, and triangles indicate respective $\nu_a(CH_2)$, $\nu_s(CH_2)$, and $\nu(COO^-)$ modes.

parameters were changed slightly. However, the calculated values did not agree with the observed ones quantitatively. This may have been because the calculation was carried out using an extreme approximation in which all interference was neglected. On the other hand, the qualitative features for the same results are summarized in Fig. 12. In this figure, all values were normalized with the reflection-absorbance of the $\nu_s(CH_2)$ mode at an angle of incidence of 30° for each polarization. With this normalization, the change in intensity of each band on the angle of incidence could be easily found. The relative band intensity was well reproduced by the non-interferential model, and the dependence of the angle of incidence was also fairly well reproduced. Although this non-interferential model is certainly an extreme approximation, we were surprised that this model could explain the

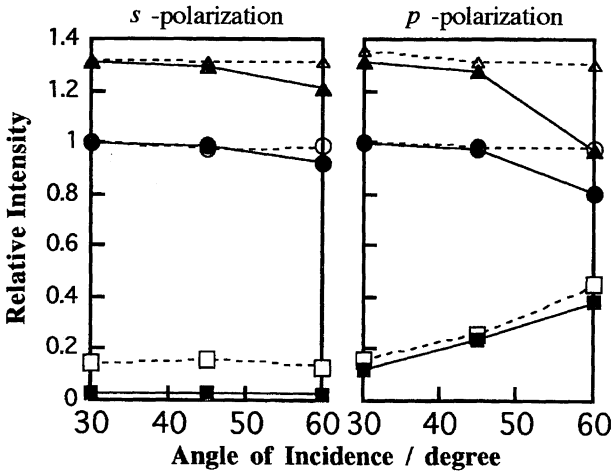

Fig. 12. Calculated (solid line) and measured (broken line) relative intensity against the angle of incidence. All values were normalized by the intensity of $\nu_s(CH_2)$ for each polarization. Squares, circles, and triangles indicate respective $\nu_a(CH_2)$, $\nu_s(CH_2)$, and $\nu_s(COO^-)$ modes. This figure is derived from Fig. 11.

entire features of the ER spectra, even with a 5-layer system calculation. At an angle of incidence of 60°, the calculated values are slightly different from the observed ones. To help speculate on this point, the figure showing the IR spots on the substrate (Fig. 13) is a good aid. Figure 13 shows incidental and emerging IR spots on the substrate (top view). At a large angle of incidental, such as 60° or larger, the centers of the IR spots are considered to be sufficiently separate from one another to prevent interference. It was then simply expected that calculations at a large angle of incidence would be closer to the observed values. In this case, however, the spots were enlarged to long ellipsoids, so that they overlapped each other. Since the enlargement factor is proportional to $\cos^{-1}\theta_i$ (θ_i is the angle of incidence), this effect will be quite big at a large angle of incidence. In this way, the non-interferential model can successively give stable results and explain the entire spectra over the wide range of the angle of incidence. Then, the effect of interference should be the major factor causing the discrepancy between the calculation and the actual ER spectra. If we can estimate the spot area ratio of the interferential and non-interferential IR rays, a quantitative predictions is possible. At present, however, such a precise estimation is too difficult. The diameters of the spots should at least be known in advance. To the best of our knowledge, although only one paper[19] contributed to an investigation of the diameter of the IR spot, it was limited under special experimental conditions. The problem of non-interference arises especially for a thick and IR-transparent substrate, both surfaces of which are finely polished. The IR window plate or ATR plate is a typical substrate that causes problems. To avoid this, one of the two surfaces of the substrate should have some roughness that can diffuse IR rays in the substrate. On this substrate, only the upper three phases (IR//air/film/substrate) can contribute to the ER spectra, and a 3-layer model should be used to analyze the ER spectra.

We then measured the FTIR ER spectra on a single-side-polished ZnSe substrate. The angle of incidence was 60° for both polarizations. The spectra for the *s*- and *p*-polar-

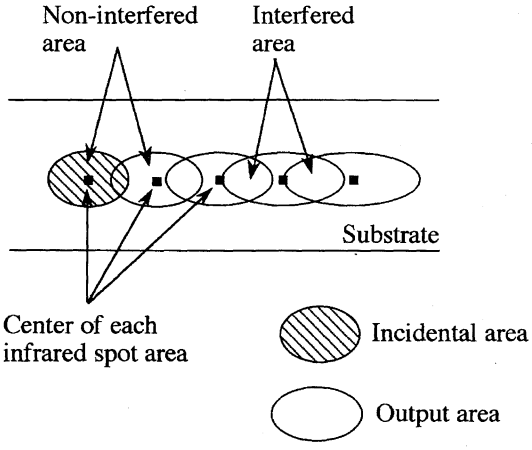

Fig. 13. A scheme for the interference of incidental beam and outputs. Crossed area represents the region of interference while the remainder is region without interference.

ization are shown in Fig. 14. These spectra clearly show that they have typical features of ER measurements for both polarizations. For a comparison, the ER spectra on a GaAs wafer were also measured. The wafer was originally made for a semiconductor device allowing IR rays to pass through. The wafer had one atomically polished surface, while the other surface was unpolished (very coarse), like the single-side-polished ZnSe plate mentioned above. The measured spectra are shown in Fig. 15. They are identical to those in a previous study[2] which are already known to be consistent with a traditional 3-layer calculation. These results proved that a prediction using the principle of interference is correct. From the above discussion we can conclude that a precise quantitative analysis of an LB film on an IR-transparent substrate with two polished sides is impossible.

In addition, the effect of the substrate surface flatness of the top side on the ER spectra was also investigated. The AFM technique showed that although the flat surface of the GaAs wafer came to be evenly covered by protrusions only 1 nm high, there were many scattered protrusions about 2 nm high. These protrusions were probably GaAs oxide. This surface pattern repeatedly appeared on the plate as domains 50—100 nm in size. Judging from the 3509-nm wavelength (2850 cm^{-1}), this roughness, or protrusion, may not be an optically serious problem in obtaining reliable spectra. The coarse surface of the GaAs wafer, on the other hand, was covered with 100-nm-high protrusions or higher. Since this roughness is comparable to one tenth of the wavelength, it could not be neglected, even optically. The *s*-polarized spectra for the two cases are shown in Fig. 16. They are apparently different from one another. Since the spectrum of Fig. 16(a) is an ordinary spectrum that is identical to that in Fig. 15(a), it is obvious that the spectrum in Fig. 16(b) is extraordinary. From these spectra, we found that the surface flatness greatly affects the ER spectra. We also investigated the other substrates used in this study. On the Ge ATR plate, protrusions 8—10 nm high were found. There were also two scratch-like structures on the surface: one was 100-nm wide and 2-nm deep; the other was 50-nm wide and 2-nm deep. These scratch-like structures may have been caused by the mechanical polishing with diamond paste. On the ZnSe ATR plate, protrusions 20—30 nm high were found. Optically, the surface roughness of these ATR plates was adequately

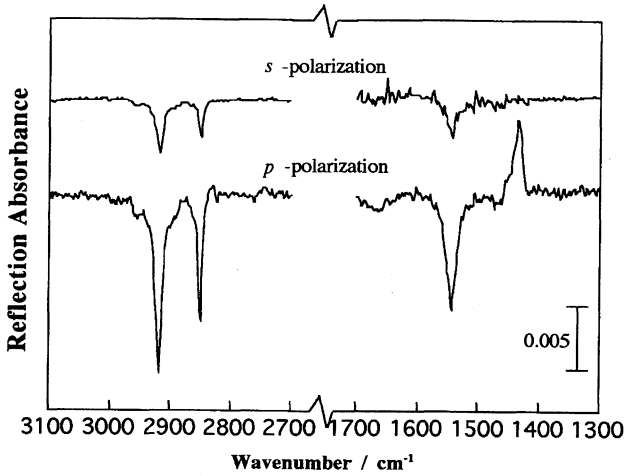

Fig. 14. Infrared ER spectra of a 9-monolayer LB film of cadmium stearate on the single-side-polished ZnSe plate. The angles of incidence were both 60°.

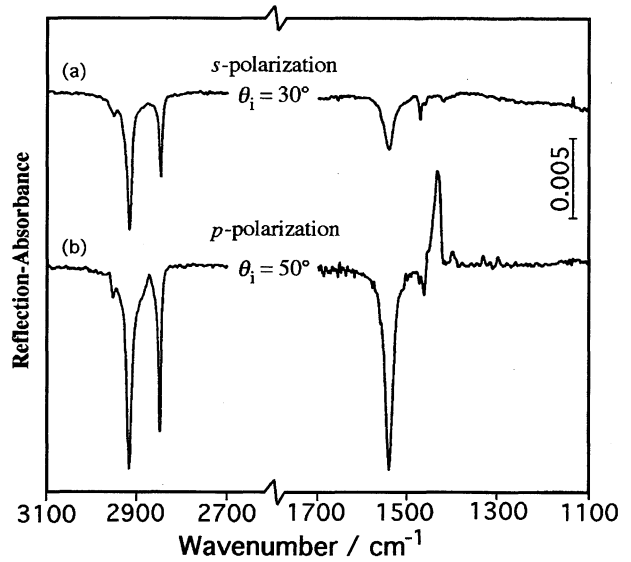

Fig. 15. Infrared ER spectra of a 9-monolayer LB film of cadmium stearate on the flat surface of a GaAs wafer.

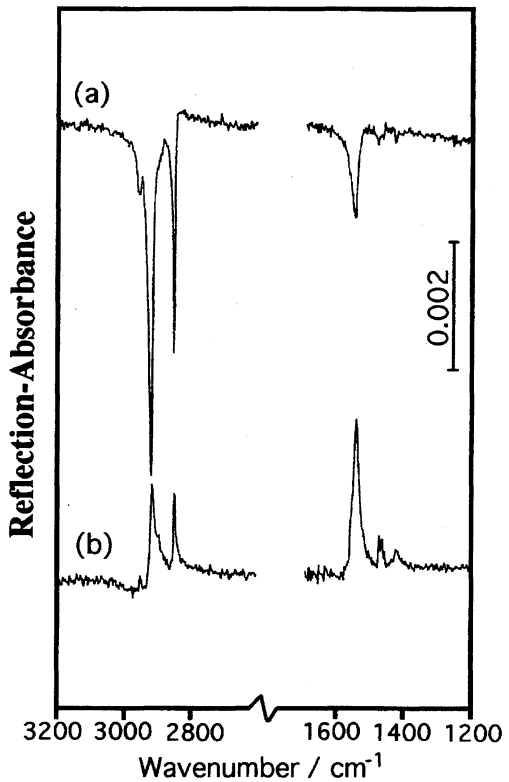

Fig. 16. The *s*-polarized infrared ER spectra of 9-monolayer LB film of cadmium stearate on a GaAs wafer with one flat surface and one coarse surface. The infrared beam was incident, at 30°, (a) on the flat surface, and (b) on the coarse surface.

small (compared to the wavelength). The thickness of the film phase (22.5 nm), however, was similar to the surface roughness of the ZnSe ATR plate. Since the spectra in Fig. 3 could be well explained by the non-interferential 5-layer model, especially the relative intensities, the roughness was found not to so seriously affect the spectra. This may have been because there were many domain structures, each of which was relatively flat over a small region.

Conclusion

The difference between the measured data and the calculated reflection-absorbances has so far been problematic. Based on our considerations in this study, non-interference of higher-order outputs was found to be the most important factor which affects measurements, making them greatly different from the conventional 5-monolayer calculation. We proved that the LB films on double-side-polished IR-transparent substrates were not suitable for precise theoretical analysis. A discussion similar to that given in this paper may be applied to transmission spectra on the same kinds of substrates when the angle of incidence is large ($\gg 0°$), since such a condition would generate multiple reflections in the substrates, thus producing non-interferential rays going to the detector. In this case, however, the amplitude of multiple reflection in the substrate would be very small, since the substrate used for the transmission measurement originally had a low reflectivity. This would be expected to help make the error in the transmission spectra much smaller than that in the ER spectra.

This work was supported by the Grant-in-Aid for Scientific Research No. 08772072 from the Ministry of Education, Science and Culture, to whom the authors' thanks are due.

References

1) A. N. Parikh and D. L. Allara, *J. Chem. Phys.*, **96**, 927 (1992).
2) T. Hasegawa, S. Takeda, A. Kawaguchi, and J. Umemura, *Langmuir*, **11**, 1236 (1995).
3) T. Hasegawa, S. R. Park, D. W. Kim, H. Lee, and J. Umemura, *Bull. Inst. Chem. Res., Kyoto Univ.*, **71**, 127 (1993).
4) J. Umemura, S. Takeda, T. Hasegawa, T. Kamata, and T. Takenaka, *Spectrochim. Acta, Part A*, **50A**, 1563 (1994).
5) W. N. Hansen, *J. Opt. Soc. Am.*, **58**, 380 (1968).
6) R. G. Greenler, *J. Chem. Phys.*, **44**, 310 (1966).
7) J. Umemura, T. Kamata, T. Kawai, and T. Takenaka, *J. Phys. Chem.*, **94**, 62 (1990).
8) J. A. Mielczarki and R. H. Yoon, *Langmuir*, **7**, 101 (1991).
9) P. Yeh, *J. Opt. Soc. Am.*, **72**, 507 (1982).
10) P. J. Lukes, M. C. Petty, and J. Yarwood, *Langmuir*, **8**, 3043 (1992).
11) F. Kimura, J. Umemura, and T. Takenaka, *Langmuir*, **2**, 96 (1986).
12) K. B. Blodgett, *J. Am. Chem. Soc.*, **56**, 495 (1934).
13) P. Drude, *Ann. Phys. Chem. N. F.*, **32**, 584 (1887).
14) K. Kudo, "Kiso Bussei Zuhyo," ("Tables for Fundamental Solid State Physics") Kyoritsu Shuppan, Tokyo (1972).
15) M.Yamamoto, "Kessyo Kogaku Hand Book," ("Handbook for Crystal Engineering,") Kyoritsu Shuppan, Tokyo (1971).
16) Y. Koga and R. Matuura, *Memo. Fac. Sci., Kyusyu Univ. Ser. C*, **4**, 1 (1961)
17) R. P. Feynman, R. B. Leighton, and M. L. Sands, "The Feynman Lectures on Physics," (Japanese version Vol. 5, "Quantum Mechanics,") Iwanami Shoten, Tokyo (1969).
18) T. Namioka, *Bunko Kenkyu (Spectroscopic Study)*, **38**, 225 (1989).
19) P. H. Axelsen, W. D. Braddock, H. L. Brockman, C. M. Jones, R. A. Dluhy, B. K. Kaufman, and F. J. Puga, II, *Appl. Spectrosc.*, **49**, 526 (1995).